J. Fluid Mech. (1992), *vol.* 236, *pp.* 111–126
Printed in Great Britain

Interfacial instabilities in aluminium reduction cells

By A. D. SNEYD
University of Waikato, Hamilton, New Zealand

(Received 3 September 1990 and in revised form 2 July 1991)

This paper extends the analysis of Sneyd (1985) on interfacial instabilities in aluminium reduction cells. The cell model consists of a plane fluid layer of relatively low electrical conductivity, sandwiched between an upper rigid wall and lower fluid layer, both of high conductivity. A steady current passes through the layers, and the magnetic field is assumed to be a linear function of position. The principal new effects introduced are (i) a horizontal current component in the aluminium; (ii) vertical magnetic field components, and vertical field gradients; (iii) an aluminium pool of finite depth; and (iv) uniform zeroth-order flow in the fluid layers, and mechanical dissipation. A dispersion relation for small-amplitude waves is derived and discussed. The destabilizing Kelvin–Helmholtz mechanism and electromagnetic forces compete with gravity, surface tension and mechanical dissipation. Electromagnetic destabilization is likely to occur in practice at wavelengths of 1 m or more, and becomes more intense with decreasing layer depths. The most dangerous mechanism appears to be driven by vertical gradients of the horizontal field.

1. Introduction

A typical aluminium reduction cell, shown schematically in figure 1(*a*), carries a current of order 10^5 A across an area of several square metres. The current enters the cell via the carbon anode, then passes through a narrow, poorly conducting layer of cryolite (a molten mixture of sodium and aluminium fluorides) which floats on a pool of liquid aluminium. The current then leaves the cell via the carbon cathode block, and is collected by a system of bus bars.

This intense current density $\boldsymbol{J}$ creates a magnetic field $\boldsymbol{B}$ and hence a Lorentz force $\boldsymbol{J}\times\boldsymbol{B}$ which has an important influence on the cell dynamics. One effect is to curve the upper free surface of the aluminium (Lympany, Evans & Moreau 1983), which makes the current distribution non-uniform. Also, if the cryolite layer is too thin it may become unstable, the aluminium rising and making contact with the carbon anode, thus short-circuiting the current path. This effect is particularly troublesome since in order to reduce the cell resistance and hence the power consumed, the cryolite layer should be as thin as possible.

The first author to analyse magnetohydrodynamic (MHD) effects in aluminium cells was Urata (1985), who calculated numerically normal modes and frequencies of electromagnetically driven waves, and applied the results to improve cell design. His work highlights the influence of cryolite layer thickness and magnetic field distribution on instability growth rates. Potočnik (1989) has also carried out numerical simulations of waves driven by Lorentz forces, and found similarly that the layer depth and field distribution are crucial factors. Both of these studies indicated that unstable modes are of relatively long wavelength – 1 m or more. Fraser, Billinghurst, Chen and Keniry (1989) have developed numerical methods for

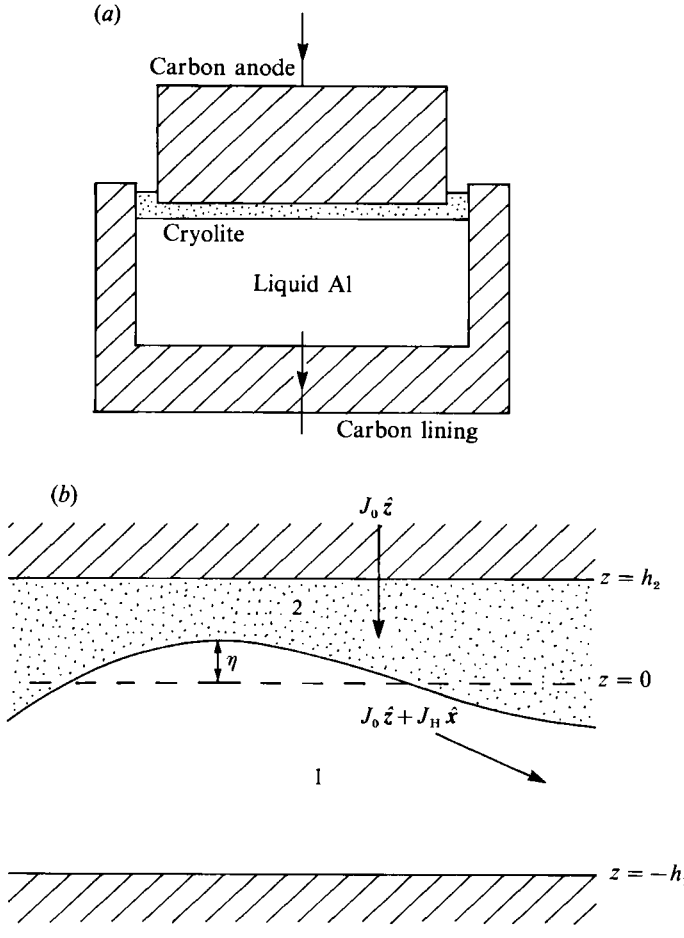

FIGURE 1. (*a*) Schematic diagram of a Hall–Héroult cell. (*b*) Diagram of the model system.

finding the electric current and magnetic field distributions within a cell, and proposed a simple model of the field distribution.

Several authors have also studied the problem analytically. Sneyd (1985) considered a model in which uniform normal current flowed through a poorly conducting fluid layer, bounded above and below by a solid (carbon) and an infinitely deep fluid layer, both of much higher conductivity. The layers were assumed to extend to infinity in the horizontal plane. The magnetic field was horizontal and a linear function of position, resolved into a component due to the local current distribution, and a far component due to remote currents such as those in the bus bars. The fluid layers were assumed plane, inviscid, and initially in hydrostatic equilibrium. It was found that the far magnetic field could drive a long-wavelength instability which became easier to trigger as the cryolite depth diminished. (We shall refer to Sneyd 1985 as paper I). Moreau & Ziegler (1986) considered a somewhat different model in which the field and current are uniform, but with a horizontal current component in the aluminium layer. Their model also includes mechanical dissipation in the fluid flow, by means of a linear frictional term. Their conclusions as regards stability are generally similar to those of paper I, but the stability mechanism seems to be somewhat different. In paper I, the essential instability

mechanism depends only on the *spatial derivatives* of the magnetic field, which are absent from the model of Moreau & Ziegler (1986).

The aim of this paper is to make the model of paper I more realistic by including several new effects believed to be important, while retaining simple analytical methods. As before the fluid layers extend to infinity horizontally, but the aluminium depth is finite. We also include horizontal current and vertical magnetic field components, but retain the assumption that the field is a linear function of position. We also abandon the assumption of initial hydrostatic equilibrium – the fluid layers now have uniform horizontal velocities – and mechanical dissipation is modelled by the linear frictional term of Moreau & Ziegler (1986). We derive a dispersion relation for waves on the cryolite–aluminium interface, which shows the effects of the new physics introduced. Since the layers are in relative motion a Kelvin–Helmholtz instability appears, while linear friction gives rise to a damping term. Mutual attraction between the horizontal current lines produces a tearing-mode-type instability, as analysed by Murty (1961). The two strongest destabilizing terms however depend only on the vertical current component. These become important only for wavelengths of order 1 m or more, and increase with decreasing layer depths. Both depend on the magnetic field gradient, the most violent instability being driven by vertical gradients of the horizontal field.

A recent study by Pigny & Moreau (1991) also analyses the effects mentioned in the previous paragraph. Their analysis is more complicated since for added realism they assume a linear spatial variation in the equilibrium electric current density $\boldsymbol{J}$. Consequently the dispersion relation obtained by Pigny & Moreau is spatially dependent, and the analysis is justified by the assumption that the lengthscale over which $\boldsymbol{J}$ varies is much greater than one wavelength. In this paper we take a simpler approach and assume at the outset that $\boldsymbol{J}$ is uniform. This gives a homogeneous dispersion relation in which all terms (with one minor exception) are constants. Slow variations in $\boldsymbol{J}$ could then be modelled by a slowly varying dispersion relation – as in ray theory.

In §2 we discuss in detail the mathematical model; §3 analyses the forces which arise from a cryolite layer perturbation, and in §4 we derive the dispersion relation. In §5 we interpret this dispersion relation, discuss its implications, and present graphs of critical Froude number versus wavelength for various magnetic field gradients and layer depths. In §6 we discuss the physical interpretation of our results, and finally, our conclusions are summarized in §7.

2. Mathematical model

In order to obtain a simple dispersion relation and to highlight the essential physics, we ignore edge effects and assume that the cryolite and aluminium layers are unbounded horizontally, occupying the regions $0 < z < h_2$, $-h_1 < z < 0$ respectively. We shall consistently use subscripts 1 and 2 to refer to variables in the cryolite and aluminium layers respectively. The region $z > h_2$ is the carbon anode, and $z < -h_1$ the carbon cathode block.

Denoting the electrical conductivity of carbon by σ_c, we assume that the ratios

$$\frac{\sigma_1}{\sigma_c}, \quad \frac{\sigma_c}{\sigma_2}$$

are both large – typically of order 10^2. Thus aluminium is a much better conductor

than carbon, which in turn is a much better conductor than cryolite. In the weakly conducting cryolite the electric current is purely vertical and we set

$$\boldsymbol{J}_2 = J_0\hat{\boldsymbol{z}}, \quad J_0 = \text{const.}$$

The assumption of constant J_0 is of course an idealization which will be invalid near the edges of the anode, where the growth of a solid cryolite ledge causes local current deviations (Fraser *et al.* 1989), but is a reasonable approximation throughout the cell interior. The highly conducting liquid aluminium generally carries a significant horizontal current, so aligning the x-axis to this component we write

$$\boldsymbol{J}_1 = J_0\hat{\boldsymbol{z}} + J_{\mathrm{H}}\hat{\boldsymbol{x}}.$$

Again our assumption of constant $\boldsymbol{J}_1$ is in reality unjustified, but necessary to obtain a simple dispersion relation. In a typical cell J_{H} may in fact change sign (Fraser *et al.* 1989) so our model will be realistic only in certain subregions. Pigny & Moreau (1991) have taken account of a linearly varying J_{H} in their analysis.

The unperturbed magnetic field satisfies

$$\nabla \times \boldsymbol{B} = \mu_0 \boldsymbol{J},$$

and we assume the simplest possible spatial dependence for $\boldsymbol{B}$ – namely linear, since $\boldsymbol{J}$ is constant. Thus we write

$$\boldsymbol{B} = \boldsymbol{\alpha} \cdot \boldsymbol{X}, \tag{2.1}$$

where $\boldsymbol{\alpha}$ is a constant second-order tensor. Since $\boldsymbol{B}$ must be continuous at $z = 0$ we insist that

$$\langle \alpha_{ij} \rangle = 0; \quad i = 1, 2, 3; \quad j = 1, 2;$$

where $\langle f \rangle = (f_1)_{z=0} - (f_2)_{z=0}$ denotes the jump in a variable across the interface. Also

$$\mu_0 \boldsymbol{J} = (\alpha_{32} - \alpha_{23},\ \alpha_{13} - \alpha_{31},\ \alpha_{21} - \alpha_{12}),$$

so

$$\langle \alpha_{13} \rangle = \langle \alpha_{31} \rangle = 0,$$

and since $\nabla \cdot \boldsymbol{B} = 0$,

$$\langle \alpha_{33} \rangle = -\langle \alpha_{11} + \alpha_{22} \rangle = 0,$$

so the only component of $\boldsymbol{\alpha}$ to be discontinuous across $z = 0$ is $\alpha_{23} = -J_{\mathrm{H}}$. Thus the tensor $\boldsymbol{\alpha}$ is conveniently written in the form

$$\boldsymbol{\alpha}_i = \mu_0 \begin{pmatrix} 0 & 0 & 0 \\ J_0 & 0 & J_{\mathrm{H}i} \\ 0 & 0 & 0 \end{pmatrix} + \mu_0 J_0 \boldsymbol{\beta}. \tag{2.2}$$

Here $J_{\mathrm{H}1} = J_{\mathrm{H}}$, $J_{\mathrm{H}2} = 0$, and $\boldsymbol{\beta}$ is a constant (dimensionless) *symmetric* tensor which represents the effect of the distant currents, such as those in the bus bars connected to anode and cathode. Note that we could also add a uniform field to the right-hand side of (2.2) but this is simply equivalent to a change of origin. Moreover, we shall show in §3 that a uniform magnetic field has no effect on the dispersion relation, apart from a gravity-like term arising from the interaction of J_x and B_y.

Flow in the aluminium and cryolite layers is turbulent, with the further complication of CO_2 bubble formation at the carbon anode, which causes inhomogeneity in density and electrical conductivity. Here we shall adopt the linear frictional equation of motion of Lympany *et al.* (1983).

$$\rho \frac{\mathrm{D}\boldsymbol{u}}{\mathrm{D}t} = -\nabla p + \boldsymbol{F} - \kappa \boldsymbol{u}, \tag{2.3}$$

where $\boldsymbol{F}$ is the body force per unit volume and κ a constant coefficient of friction to model the dissipative effects of viscosity and turbulence. This drastic simplification can be justified by integrating across the layer the Navier–Stokes equations for the nearly horizontal flow, and appears to work well in practice (Lympany *et al.* 1983).

It should be emphasized that we make no attempt to solve the equations of motion in the unperturbed state. This would be a difficult task since the flow is turbulent and largely controlled by conditions in the channels surrounding the anodes, so we simply assume that some unperturbed state exists. We also assume that in the region being analysed, the horizontal unperturbed flow $\boldsymbol{u} = \boldsymbol{U}_i$, $i = 1, 2$, is uniform in the two fluid layers. Our analysis thus provides no theoretical estimate of the $\boldsymbol{U}_i$, and when presenting results we assume measured experimental values.

A final approximation is that the magnetic diffusion time is short compared with a wave period (or growth time of an instability) so that current and magnetic field perturbations can be calculated using static methods. This assumption can be justified *a posteriori* (paper I).

3. Forces due to interfacial perturbation

3.1. *Current perturbation*

Imagine that the cryolite/aluminium interface suffers a perturbation

$$z = \eta = \eta_0 \mathrm{e}^{\mathrm{i}\chi}, \quad \chi = \boldsymbol{k}\cdot\boldsymbol{X} - \omega t, \tag{3.1}$$

where η_0 is a (small) constant, and $\boldsymbol{k} = (l, m, 0)$ is a horizontal wavenumber vector. Current now tries to flow through the narrowest part of the poorly conducting cryolite layer, and we calculate the perturbation using Ohm's law and the electrostatic approximation:

$$\boldsymbol{J} = \sigma \boldsymbol{E}, \quad \nabla \times \boldsymbol{E} = 0.$$

Thus the current perturbation $\boldsymbol{j}_i$ in either layer can be written in the form

$$\boldsymbol{j}_i = \nabla \phi_i, \quad \text{where} \quad \nabla^2 \phi_i = 0.$$

Introducing the harmonic functions

$$H^+ = \mathrm{e}^{kz}\mathrm{e}^{\mathrm{i}\chi}, \quad H^- = \mathrm{e}^{-kz}\mathrm{e}^{\mathrm{i}\chi}$$

we write

$$\phi_i = \alpha_i^+ H^+ + \alpha_i^- H^-, \quad i = 1, 2,$$

where the $\alpha_i^{\pm}$ are constant coefficients to be determined.

The anode boundary $z = h_2$ is highly conducting in comparison with cryolite, so here ϕ_2 must be constant:

$$\alpha_2^+ \mathrm{e}^{K_2} + \alpha_2^- \mathrm{e}^{-K_2} = 0, \tag{3.2}$$

where $K_i = kh_i$. On the other hand, the cathode block $z = -h_1$ is insulating in comparison with aluminium, and here the normal component of the current perturbation must vanish:

$$\alpha_1^+ \mathrm{e}^{-K_1} - \alpha_1^- \mathrm{e}^{K_1} = 0. \tag{3.3}$$

At $z = 0$ we invoke continuity of normal current, and constancy of ϕ_2 at the highly conducting aluminium interface:

$$\alpha_2^+ - \alpha_2^- = \alpha_1^+ - \alpha_1^- - \mathrm{i}J_{\mathrm{H}}\eta_0 l/k, \tag{3.4}$$

$$\alpha_2^+ + \alpha_2^- + J_0\eta_0 = 0. \tag{3.5}$$

A more detailed discussion of the boundary conditions for arbitrary layer

conductivities is given in the Appendix. This further justifies the approximate conditions (3.2)–(3.5).

Solving (3.2)–(3.5) for the coefficients yields

$$\alpha_2^+ = \tfrac{1}{2}J_0\,\eta_0(\mathscr{C}_2-1), \quad \alpha_2^- = -\tfrac{1}{2}J_0\,\eta_0(\mathscr{C}_2+1), \tag{3.6a, b}$$

$$\alpha_1^+ = \tfrac{1}{2}\eta_0\left(J_0\mathscr{C}_2+\frac{\mathrm{i}J_{\mathrm{H}}\,l}{k}\right)(\mathscr{C}_1+1), \quad \alpha_1^- = \tfrac{1}{2}\eta_0\left(J_0\mathscr{C}_2+\frac{\mathrm{i}J_{\mathrm{H}}\,l}{k}\right)(\mathscr{C}_1-1), \tag{3.6c, d}$$

where $\mathscr{C}_i = \coth(K_i)$.

3.2. *Magnetic field perturbation*

We write the magnetic field perturbation $\boldsymbol{b}_i$ in each layer in the form

$$\boldsymbol{b}_i = \boldsymbol{b}_{\mathrm{A}i}+\boldsymbol{b}_{\mathrm{P}i}, \quad i = 1, 2,$$

where $\boldsymbol{b}_{\mathrm{A}}$ satisfies Ampères law, and $\boldsymbol{b}_{\mathrm{P}}$ is an irrotational correction necessary to ensure continuity at $z = \eta$. We can set

$$\boldsymbol{b}_{\mathrm{A}i} = \frac{\mu_0}{k}(\nabla\phi_i^- - \nabla\phi_i^+)\times\hat{\boldsymbol{z}}, \tag{3.7}$$

and it is easily verified that

$$\nabla\cdot\boldsymbol{b}_{\mathrm{A}i} = 0, \quad \nabla\times\boldsymbol{b}_{\mathrm{A}i} = \mu_0\boldsymbol{j}_i, \quad i = 1, 2.$$

Since the magnetic field is continuous across $z = \eta$,

$$(\boldsymbol{B}_1+\boldsymbol{b}_1)_{z=\eta} = (\boldsymbol{B}_2+\boldsymbol{b}_2)_{z=\eta},$$

which to leading order in η_0 yields

$$(\boldsymbol{b}_1)_{z=0} - (\boldsymbol{b}_2)_{z=0} = \eta\left(\frac{\partial\boldsymbol{B}_2}{\partial z}-\frac{\partial\boldsymbol{B}_1}{\partial z}\right)_{z=0},$$

or using (2.2),

$$\langle\boldsymbol{b}\rangle = \mu_0 J_{\mathrm{H}}\,\eta\hat{\boldsymbol{y}}. \tag{3.8}$$

Equation (3.7) can be written in the form,

$$\boldsymbol{b}_{\mathrm{A}i} = \frac{\mathrm{i}\mu_0}{k^2}j_{zi}\boldsymbol{k}\times\hat{\boldsymbol{z}} \quad \text{or} \quad \langle\boldsymbol{b}_{\mathrm{A}}\rangle = \frac{\mathrm{i}\mu_0}{k^2}\langle j_z\rangle\boldsymbol{k}\times\hat{\boldsymbol{z}}. \tag{3.9}$$

Continuity of normal current at $z = \eta$ shows that $\langle j_z\rangle = \mathrm{i}J_{\mathrm{H}}\,l\eta$ (cf. 3.4), and substitution into (3.9) yields

$$\langle\boldsymbol{b}_{\mathrm{A}}\rangle = \frac{-\mu_0 J_{\mathrm{H}}\,l\eta}{k^2}\boldsymbol{k}\times\hat{\boldsymbol{z}}. \tag{3.10}$$

Now combining (3.8) and (3.10) we find

$$\langle\boldsymbol{b}_{\mathrm{P}}\rangle = \frac{\mu_0 J_{\mathrm{H}}\,m\,\eta\boldsymbol{k}}{\boldsymbol{k}^2}. \tag{3.11}$$

Note that since j_z is continuous across the plane interfaces $z = h_2$ and $z = -h_1$, (3.9) shows that $\boldsymbol{b}_{\mathrm{A}}$ is likewise continuous, so the only discontinuity in $\boldsymbol{b}_{\mathrm{P}}$ is across $z = \eta$. To find the (unique) irrotational and solenoidal $\boldsymbol{b}_{\mathrm{P}}$ which satisfies (3.11) and vanishes at $z = \pm\infty$, we set

$$\boldsymbol{b}_{\mathrm{P}1} = \nabla(aH^+), \quad \boldsymbol{b}_{\mathrm{P}2} = -\nabla(aH^-).$$

The constant a is determined from (3.11) to be

$$a = -\mathrm{i}\mu_0 J_{\mathrm{H}} \eta_0 m/2k^2. \tag{3.12}$$

3.3. *Lorentz force perturbation*

The Lorentz-force perturbation $\boldsymbol{F}$ is given by

$$\boldsymbol{F} = \boldsymbol{j}\times\boldsymbol{B} + \boldsymbol{J}\times\boldsymbol{b}.$$

Since $\nabla\times\boldsymbol{b}_{\mathrm{P}} = 0$, we can write

$$\boldsymbol{F} = \frac{1}{\mu_0}[(\nabla\times\boldsymbol{b}_{\mathrm{A}})\times\boldsymbol{B} + (\nabla\times\boldsymbol{B})\times\boldsymbol{b}_{\mathrm{A}}] + \boldsymbol{J}\times\boldsymbol{b}_{\mathrm{P}} = \boldsymbol{F}_{\mathrm{A}} + \boldsymbol{F}_{\mathrm{P}} - \nabla p_{\mathrm{M}},$$

where

$$\boldsymbol{F}_{\mathrm{A}} = \frac{1}{\mu_0}[(\boldsymbol{B}\cdot\nabla)\boldsymbol{b}_{\mathrm{A}} + (\boldsymbol{b}_{\mathrm{A}}\cdot\nabla)\boldsymbol{B}], \quad \boldsymbol{F}_{\mathrm{P}} = \boldsymbol{J}\times\boldsymbol{b}_{\mathrm{P}},$$

and $p_{\mathrm{M}} = \boldsymbol{B}\cdot\boldsymbol{b}_{\mathrm{A}}$ is a magnetic pressure term. It turns out when calculating the dispersion relation that the essential information is the divergence and vertical components of $\boldsymbol{F}_{\mathrm{A}} + \boldsymbol{F}_{\mathrm{P}}$. The magnetic pressure term is simply incorporated into the fluid pressure.

Since $\nabla\cdot\boldsymbol{F}_{\mathrm{P}} = 0$ we need only consider the divergence of $\boldsymbol{F}_{\mathrm{A}}$, given by

$$\nabla\cdot\boldsymbol{F}_{\mathrm{A}} = \frac{2}{\mu_0}\frac{\partial b_{\mathrm{A}i}}{\partial x_j}\frac{\partial B_j}{\partial x_i},$$

where the suffixes denote components (not layers) and the summation convention has been used. Alternatively, using tensor notation we can write

$$\nabla\cdot\boldsymbol{F}_{\mathrm{A}} = \frac{2}{\mu_0}(\nabla\boldsymbol{B})^{\mathrm{T}} : \nabla\boldsymbol{b} = \frac{2}{\mu_0}\boldsymbol{\alpha}^{\mathrm{T}} : \nabla\boldsymbol{b}. \tag{3.13}$$

We then find, using (2.2) and (3.7), that

$$\nabla\cdot\boldsymbol{F}_{\mathrm{A}i} = \eta_0(d_i^+ H^+ + d_i^- H^-), \tag{3.14}$$

where the constant coefficients $d^{\pm}$ are given by

$$d_i^+ = \frac{2\mu_0 J_0}{k}(\mathrm{i}\beta_{\mathrm{V}} - \beta_{\mathrm{H}})\alpha_i^+, \quad d_i^- = \frac{2\mu_0 J_0}{k}(\mathrm{i}\beta_{\mathrm{V}} + \beta_{\mathrm{H}})\alpha_i^-, \tag{3.15}$$

where

$$\beta_{\mathrm{H}} = m^2 + lm(\beta_{11} - \beta_{22}) + \beta_{12}(m^2 - l^2), \quad \beta_{\mathrm{V}} = k(m\beta_{13} - l\beta_{23}). \tag{3.16a, b}$$

Thus the coefficient β_{H} depends purely on the horizontal magnetic field components and their horizontal derivatives, while β_{V} depends on vertical components or derivatives of the far field.

Since $\boldsymbol{b}_{\mathrm{A}}$ is horizontal,

$$f_{\mathrm{A}z} = \frac{1}{\mu_0}(\boldsymbol{b}_{\mathrm{A}}\cdot\nabla)B_z,$$

and since the only horizontal component of $\boldsymbol{J}$ is J_x,

$$f_{\mathrm{P}z} = J_z b_{\mathrm{P}} y.$$

Using (2.2), (3.7) and (3.12) we find

$$(\boldsymbol{F}_{\mathrm{A}i} + \boldsymbol{F}_{\mathrm{P}i})_z = \eta_0(V_i^+ H^+ + V_i^- H^-), \quad i = 1, 2, \tag{3.17}$$

where the coefficients $V_i^{\pm}$ are given by

$$V_1^{\pm} = \pm\frac{i\mu_0 J_0}{k^2}\alpha^{\pm}\beta_V, \quad V_2^{-} = \frac{-im\mu_0 J_0}{k^2}\alpha_2^{-}\beta_V, \tag{3.18a, b}$$

$$V_2^{+} = \frac{i\mu_0 J_0}{k^2}\alpha_2^{+}\beta_V + \frac{\mu_0 J_H^2 m^2}{2k^2}. \tag{3.18c}$$

The final term in V_2^+ is the only manifestation of $\boldsymbol{b}_P$.

It is interesting to note that all the essential coefficients $d_i^{\pm}$, $V_i^{\pm}$ depend only on the gradients of $\boldsymbol{B}$. The presence of an additional uniform magnetic field would therefore not change the expressions (3.18).

4. Dispersion relation

4.1. *Pressure perturbation*

Linearizing (2.3) we find that the fluid velocity perturbation $\boldsymbol{u}$ satisfies

$$\rho_i\left[\frac{\partial \boldsymbol{u}_i}{\partial t} + (\boldsymbol{U}_i\cdot\nabla)\boldsymbol{u}_i\right] = -\nabla p_i + \boldsymbol{F}_{Ti} - \kappa_i \boldsymbol{u}_i, \quad i = 1, 2,$$

where $p_i = p_{Mi}$ plus the fluid pressure perturbation, and $\boldsymbol{F}_T = \boldsymbol{F}_A + \boldsymbol{F}_P$. We assume that $\boldsymbol{u}_i$, like all other perturbed variables, is proportional to e^{ix}, so that

$$\rho_i(i\Omega_i + \kappa_i)\boldsymbol{u}_i = -\nabla p_i + \boldsymbol{F}_{Ti}, \tag{4.1}$$

where

$$\Omega_i = \omega + \boldsymbol{k}\cdot\boldsymbol{U}_i. \tag{4.2}$$

Since the flow is assumed incompressible, the divergence of (4.1) gives

$$\nabla^2 p_i = \nabla\cdot\boldsymbol{F}_{Ti}. \tag{4.3}$$

Using (3.14), and noting that $\nabla^2(zH^{\pm}) = \pm 2kH^{\pm}$, the solution for p_i of (4.3) can be written in the form

$$p_i = \frac{\eta_0}{2k}(d_i^{+} zH^{+} - d_i^{-} zH^{-} + A_i^{+} H^{+} + A_i^{-} H^{-}), \tag{4.4}$$

where the four arbitrary constants $A_i^{\pm}$ can be determined from the kinematic boundary conditions at the interfaces.

At the rigid surfaces $z = h_2$, $z = -h_1$ the normal component of $\boldsymbol{u}$ must vanish, and applying (4.1) and (3.17) we find

$$\left(\frac{\partial p_2}{\partial z}\right)_{z=h_2} = \eta_0(V_2^{+} H^{+} + V_2^{-} H^{-})_{z=h_2}, \tag{4.5}$$

$$\left(\frac{\partial p_1}{\partial z}\right)_{z=-h_1} = \eta_0(V_1^{+} H^{+} + V_1^{-} H^{-})_{z=-h_1}. \tag{4.6}$$

At the aluminium/cryolite interface $z = \eta$,

$$\frac{D}{Dt}(\eta - z) = 0 \quad \text{or} \quad \frac{D\eta}{Dt} = u_z.$$

Applying this condition on either side of the interface, and using (4.1) and (3.17) we obtain

$$\left(\frac{\partial p_i}{\partial z}\right)_{z=0} = \eta_0(V_i^{+} H^{+} + V_i^{-} H^{-})_{z=0} - i\eta_0\Omega_i(i\rho_i\Omega_i + \kappa_i), \quad i = 1, 2. \tag{4.7}$$

The four equations (4.5)–(4.7) now determine the constants $A_i^{\pm}$. The essential information needed for the dispersion relation is the pressure perturbations on either side of the interface, i.e. $A_i^+ + A_i^-$. After a little algebra one finds

$$A_1^+ + A_1^- = 2(V_1^+ - V_1^-) - \frac{1}{k}(d_1^+ + d_1^-) + h_1 d_1^+(\mathscr{C}_1 - 1) + h_1 d_1^-(\mathscr{C}_1 + 1) + 2\mathscr{C}_1(\rho_1 \Omega_1^2 - \mathrm{i}\kappa_1 \Omega_1). \tag{4.8}$$

To write the corresponding equation for layer 2, just replace the suffix 1 by 2, and $\mathscr{C}_1$ by $-\mathscr{C}_2$.

4.2. *Dispersion relation*

Now that the various perturbations have been calculated, we obtain the dispersion relation by applying the dynamic condition at $z = \eta -$ that the jump in p is balanced by surface tension. Thus, to first order in η_0,

$$p_2 + \eta\left(\frac{\partial P_2}{\partial z}\right)_{z=0} - p_1 - \eta\left(\frac{\partial P_1}{\partial z}\right)_{z=0} = \gamma \nabla^2 \eta, \tag{4.9}$$

where P_1 and P_2 are the zeroth-order pressures in the two layers, and γ is the coefficient of surface tension. In the unperturbed state the fluid velocity is horizontal, so there exists a vertical hydrostatic equilibrium,

$$\frac{\partial P_i}{\partial z} = F_i$$

where $\boldsymbol{F}$ is the unperturbed body force. The electric current in the cryolite layer is purely vertical, so $F_{z2} = -\rho_2 g$, but the horizontal current in the aluminium gives

$$F_{z1} = -\rho_1 g - J_{\mathrm{H}} B_y,$$

so that

$$\left(\frac{\partial P_2}{\partial z} - \frac{\partial P_1}{\partial z}\right)_{z=0} = g\Delta\rho + J_{\mathrm{H}} B_y, \tag{4.10}$$

where $\Delta\rho = \rho_1 - \rho_2$. Now using (4.4), (4.8) and (4.10), the dispersion relation (4.9) can be written in the form

$$\mathscr{C}_1 \Omega_1(\rho_1 \Omega_1 - \mathrm{i}\kappa_1) + \mathscr{C}_2 \Omega_2(\rho_2 \Omega_2 - \mathrm{i}\kappa_2) = \gamma k^3 + k(g\Delta\rho + J_{\mathrm{H}} B_y) + V_2^+ - V_2^- - V_1^+ + V_1^-$$
$$+ \frac{1}{2k}(d_1^+ + d_1^- - d_2^+ - d_2^-) - \tfrac{1}{2}h_2[d_2^+(\mathscr{C}_2 + 1) + d_2^-(\mathscr{C}_2 - 1)] - \tfrac{1}{2}h_1[d_1^+(\mathscr{C}_1 - 1) + d_1^-(\mathscr{C}_1 + 1)].$$

Finally substituting the expressions for $d_i^{\pm}$, $V_i^{\pm}$ given by (3.15) and (3.18) we obtain,

$$\mathscr{C}_1 \Omega_1(\rho_1 \Omega_1 - \mathrm{i}\kappa_1) + \mathscr{C}_2 \Omega_2(\rho_2 \Omega_2 - \mathrm{i}\kappa_2) = \gamma k^3 + k(g\Delta\rho + J_{\mathrm{H}} B_y) + M_1 + M_2 - M_3, \tag{4.11}$$

where the magnetic terms are given by

$$M_1 = \mu_0 J_0^2 \left[\frac{h_2 \beta_{\mathrm{H}}}{k \sinh^2 K_2} - \frac{\mathrm{i}h_1 \beta_{\mathrm{V}} \mathscr{C}_2}{k \sinh^2 K_1}\right], \tag{4.12a}$$

$$M_2 = \mu_0 J_0 J_{\mathrm{H}} \left[\frac{h_1 \beta_{\mathrm{V}} l}{k^2 \sinh^2 K_1} - \frac{\mathrm{i}\beta_{\mathrm{H}} l}{k^3}\right], \quad M_3 = \frac{\mu_0 J_{\mathrm{H}}^2 m^2}{2k^2}. \tag{4.12b, c}$$

This derivation is strictly valid only if B_y is independent of x and y, since throughout the calculation both ω and k have been treated as constants. In general B_y will not be constant, but we show in the next section that its effect is small

compared with the dominant magnetic terms, so any inconsistency is unimportant. We note that this is the only term in the dispersion relation which is affected by the presence of a uniform magnetic field – all other magnetic terms depend on the field gradient.

5. Interpretation of results

5.1. *Special cases*

If we set J_0, U_i and κ_i all equal to zero in (4.11) we obtain the dispersion relation

$$(\rho_1 \mathscr{C}_1 + \rho_2 \mathscr{C}_2)\omega^2 = gk\Delta\rho + \gamma k^3.$$

This is just the dispersion relation for capillary–gravity waves at the interface between two fluid layers. Since cryolite is less dense than aluminium, $\Delta\rho > 0$, so gravity and surface tension are both stabilizing.

If we set $J_H = 0$ (electric current purely vertical), $h_1 = \infty$ (aluminium pool infinitely deep) and take U_i and κ_i to be zero (ideal fluids initially in equilibrium), we recover the model considered in paper I. The dispersion relation (4.11) reduces to

$$(\rho_1 + \mathscr{C}_2 \rho_2)\,\omega^2 = \gamma k^3 + \Delta\rho g k + \frac{\mu_0 J_0^2 h_2 \beta_H}{k \sinh^2 K_2}, \tag{5.1}$$

which is equivalent to (3.11) of paper I. The expression (3.16a) for β_H can be written in the form

$$\beta_H = m^2 + \tfrac{1}{2}k^2 \sin(2\theta)\,(\lambda_1 - \lambda_2), \tag{5.2}$$

where the λ_i are the (real) eigenvalues of the symmetric 2×2 matrix (β_{ij}), $1 \leqslant i,j \leqslant 2$, and θ is the angle between one of the principal axes of this matrix and the wavenumber vector $\boldsymbol{k}$. As discussed in paper I the local magnetic field, represented by the first term on the right-hand size of (5.2), is always stabilizing, but remaining far-field terms may lead to a negative and destabilizing β_H. This term represents a potentially dangerous instability, since $h_2/\sinh^2 K_2$ becomes unbounded as $h_2 \to 0$. Thus if the far-field gradients yield a negative β_H, instability will always occur if the cryolite layer is sufficiently thin. We shall call this mechanism, the basic instability.

Note that the basic instability can be eliminated if the matrix (β_{ij}) is isotropic, so that $\lambda_1 = \lambda_2$. The implication for aluminium cell design is that the current distribution should be arranged as symmetrically as possible.

5.2. *General case*

To analyse the dispersion relation in more detail, we write the solution of (4.11) for ω in the form

$$\omega = \frac{\mathrm{i}\kappa - \boldsymbol{k}\cdot(\rho_1 \mathscr{C}_1 \boldsymbol{U}_1 + \rho_2 \mathscr{C}_2 \boldsymbol{U}_2) \pm \Delta^{\frac{1}{2}}}{\rho_1 \mathscr{C}_1 + \rho_2 \mathscr{C}_2}, \tag{5.3}$$

where $2\kappa = \mathscr{C}_1 \kappa_1 + \mathscr{C}_2 \kappa_2$ and the discriminant Δ is given by

$$\Delta = R(\rho_1 \mathscr{C}_1 + \rho_2 \mathscr{C}_2) - \rho_1 \rho_2 \mathscr{C}_1 \mathscr{C}_2 \delta_u^2 - \kappa^2 + \mathrm{i}\mathscr{C}_1 \mathscr{C}_2 \delta_u (\rho_2 \kappa_1 - \rho_1 \kappa_2). \tag{5.4}$$

In (5.4) we have used the abbreviation $\delta_u = \boldsymbol{k}\cdot(\boldsymbol{U}_1 - \boldsymbol{U}_2)$; R denotes the right-hand side of the dispersion (4.11). The obvious fluid dynamic effects are stabilization by the linear frictional term $\mathrm{i}\kappa$, and destabilization by the Kelvin–Helmholtz term $-\rho_1 \rho_2 \mathscr{C}_1 \mathscr{C}_2 \delta_u^2$.

The magnetic terms of R will be destabilizing if negative or complex. The real part M_{1R} say of M_1 (equation (4.12a)) represents the basic mechanism discussed in paper I. The term M_3 involving J_H^2 is always destabilizing, and represents the pinching

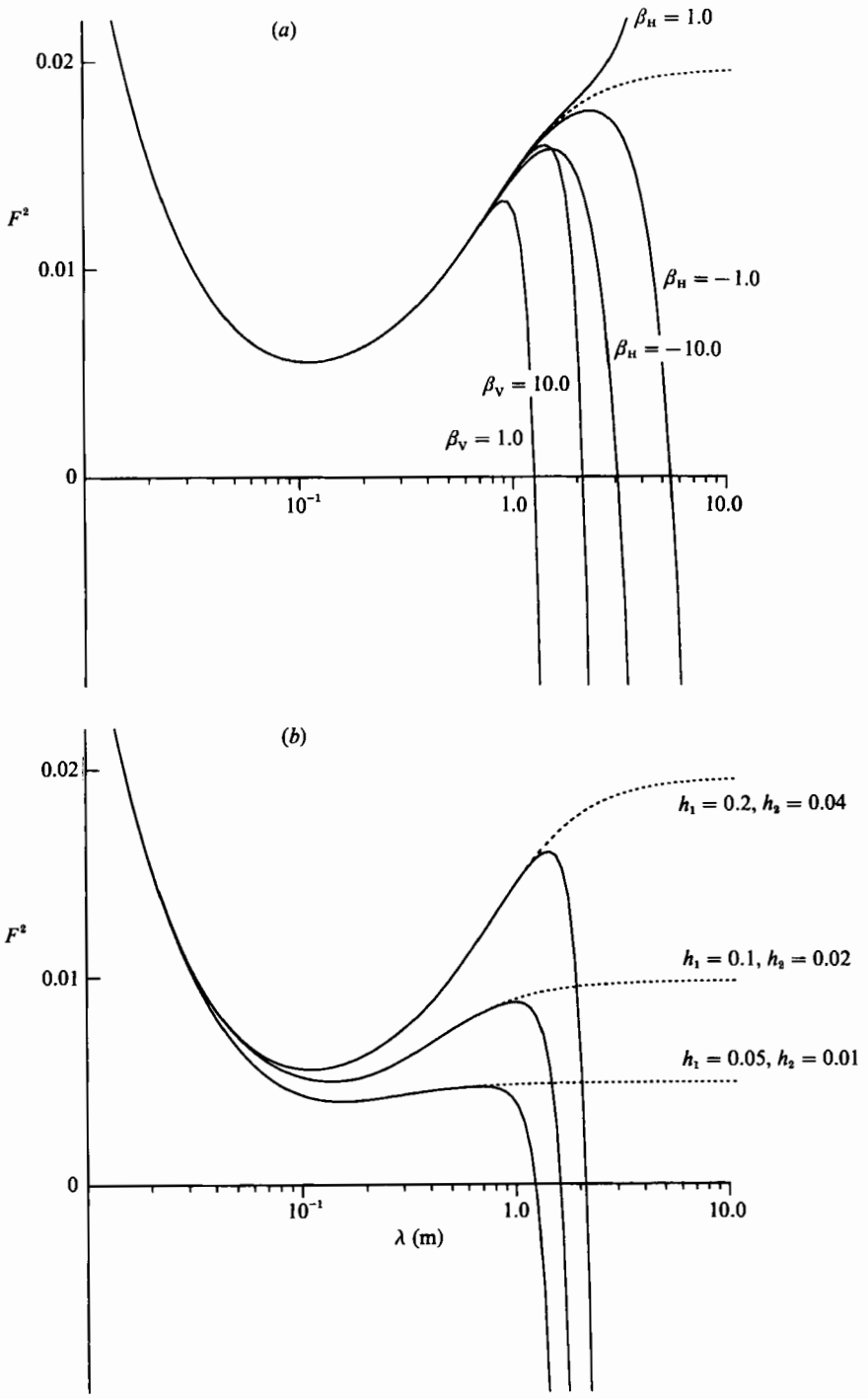

FIGURE 2. Graphs of critical Froude number F^2 versus wavelength λ. The parameters J_0, $\Delta\rho$, and γ assume typical values given in §5.2. The dashed curve represents the pure Kelvin–Helmholtz instability in the absence of electromagnetic effects. In (*a*) $h_2 = 4$ cm, $h_1 = 20$ cm and the values of β_H, β_V are varied separately. (Only one of β_H, β_V is non-zero for any given curve.) In (*b*) $\beta_H = -1$, $\beta_V = 1$ and the layer depths are varied. Note that the wavelength scale is logarithmic.

effect of the mutually attracting horizontal currents (or tearing mode), as analysed by Murty (1961). The imaginary terms $M_{1\mathrm{I}}$ and $M_{2\mathrm{I}}$ may give rise to negative imaginary parts in ω which will also be destabilizing.

To compare relative magnitudes of gravity, surface tension, and magnetic components of R we define dimensionless numbers

$$N_M = \frac{\mu_0 J_0^2 L}{\Delta\rho g}, \quad N_\gamma = \frac{\gamma}{L^2 \Delta\rho g},$$

where L is a horizontal lengthscale of the cell. We have assumed $k = O(L^{-1})$ since it is apparent from (4.12) that the longest wavelengths are most prone to magnetic destabilization. Using typical values in SI units, $J_0 = 10^4$, $\Delta\rho = 1.82 \times 10^2$, $g = 9.81$, $L = 1$, $\gamma = 0.5$, we find

$$N_M = 7.0 \times 10^{-2}, \quad N_\gamma = 2.7 \times 10^{-3}.$$

Thus the surface tension is negligible for the longest wavelengths. Furthermore M_2, M_3 and the gravity-type term $J_{\mathrm{H}} B_y$ in (4.11) are of order N_M compared to $k\Delta\rho g$, and may also be neglected, to good approximation. The term M_1 however depends on the depths of the aluminium and cryolite layers:

$$\frac{M_{1\mathrm{R}}}{k\Delta\rho g} \approx \frac{N_M L}{h_2}, \quad \frac{M_{1\mathrm{I}}}{k\Delta\rho g} \approx \frac{N_M L^2}{h_1 h_2}.$$

We have assumed $K_1, K_2 \ll 1$, which is reasonable since in a typical cell, $h_1 = 20$ cm and $h_2 = 4$ cm, compared with the horizontal lengthscale of 1 m. Thus we see that $M_{1\mathrm{R}}$ and $M_{1\mathrm{I}}$ are comparable or even somewhat larger than gravity. The most dangerous term seems to be $M_{1\mathrm{I}}$, which is proportional to β_{V}; thus vertical magnetic field gradients play a vital role. It is interesting that both $M_{1\mathrm{R}}$ and $M_{1\mathrm{I}}$ are independent of the horizontal current component J_{H}, which appears only in the lower-order magnetic terms.

To present our results graphically we follow Moreau & Ziegler (1986), and define a Froude number F by setting

$$F^2 = \frac{\delta_u^2}{gLk^2};$$

then plot the value of F^2 giving neutral stability against wavelength $\lambda = 2\pi/k$. The neutral curves $\mathrm{Im}\,(\omega) = 0$ separate the (λ, F^2)-plane into unstable and stable regions. The dashed curve is the boundary in the absence of magnetic forces ($\beta_{\mathrm{H}} = \beta_{\mathrm{V}} = 0$), which is similar to the usual Kelvin–Helmholtz curve but slightly modified by frictional damping. To illustrate the separate effects of horizontal and vertical magnetic field gradients, the parameters β_{H} and β_{V} have been varied in figure 2(*a*) – one parameter being set equal to zero as the other is varied. It can be seen that magnetic effects are important only for wavelengths of order 1 m or more. The effect of β_{H} depends upon its sign, positive values being stabilizing and negative values destabilizing. The term β_{V} is always destabilizing – more dramatically so than β_{H}, as predicted above. Figure 2(*b*) also shows that decreasing the layer depths h_1 and (particularly) h_2 makes the system more susceptible to magnetic instabilities. For the curves in figure 2, only the dominant magnetic term M_1 has been included in the calculation.

6. Physical interpretation

The interplay of physical effects considered in the last section is difficult to unravel, and the aim of this section is to describe just one simple mechanism for electromagnetic destabilization.

We consider a disturbance propagating in the x-direction so that the wavenumber vector $\boldsymbol{k} = (l, 0, 0)$. We also assume that there is no horizontal current, $J_{\mathrm{H}} = 0$, and that the only non-vanishing components of the tensor $\boldsymbol{\beta}$ are

$$\beta_{12} = \beta_{21} = \beta \quad \text{(say)} \quad > 0.$$

Equation (3.16) thus gives $\beta_{\mathrm{H}} = -l^2\beta$, which is negative and destabilizing. Equations (2.1) and (2.2) give

$$\boldsymbol{B} = \mu_0 J_0(\beta y, (1+\beta)x, 0). \tag{6.1}$$

We assume zero mean flow and ignore the frictional term, setting $\boldsymbol{U}_i = 0$ and $\kappa = 0$.

Figure 3 shows the field lines of the perturbation current $\boldsymbol{j}$, calculated using the formulae in §3. If the perturbation is unstable, we would expect the circulation Γ around the closed loop $ABCD$ in the figure,

$$\Gamma = \int_{ABCD} \boldsymbol{u}\cdot \mathrm{d}\boldsymbol{x},$$

to be positive – i.e. in the sense indicated by the double arrows. The fluid would then be rising where the interface is elevated, and falling where it is depressed. Integrating the equation of motion (2.3) around $ABCD$ eliminates the pressure and gives

$$\frac{\mathrm{d}\Gamma}{\mathrm{d}t} = \frac{1}{\rho}\int_{ABCD} \boldsymbol{F}\cdot \mathrm{d}\boldsymbol{x}. \tag{6.2}$$

If the disturbance is therefore to grow, the body forces $\boldsymbol{F}$ must generate positive vorticity inside $ABCD$.

Considering the first term, $\boldsymbol{j}\times\boldsymbol{B}$, of the Lorentz-force perturbation, we find

$$[\nabla\times(\boldsymbol{j}\times\boldsymbol{B})]_y = [-(\boldsymbol{j}\cdot\nabla)\boldsymbol{B}]_y = -j_x\mu_0 J_0(1+\beta)$$

using (6.1). Since $J_0 < 0$ (the current is flowing down from the anode) we can apply Stokes's theorem to (6.2) and write

$$\frac{\mathrm{d}\Gamma}{\mathrm{d}t} = \int_R cj_x \,\mathrm{d}x\,\mathrm{d}z, \tag{6.3}$$

where R is the interior of $ABCD$ and c a positive constant. It can be seen in figure 3 that $j_x < 0$ for $y > 0$ while $j_x > 0$ for $y < 0$. Clearly, however, the positive contributions to the integral in (6.3) will overwhelm the negative contributions, since the aluminium ($y < 0$) includes the return path of the current, where $\boldsymbol{j}$ is almost horizontal and in the positive x-direction. In the cryolite on the other hand $\boldsymbol{j}$ is nearly vertical, and $|j_x|$ is smaller, so the negative contributions from this region are less important. (This can be confirmed by an exact integration, using the formulae for $\boldsymbol{j}$ in §3.) The current circuit for $\boldsymbol{j}$ is of course completed in the anode, which has much greater conductivity than the cryolite. The conclusion from (6.3) is therefore that Γ will be positive and destabilizing.

The second Lorentz-force term, $\nabla(\boldsymbol{J}\times\boldsymbol{b})$, may be stabilizing, but is independent of the far-field gradient β. In (6.3) the constant $c = \mu_0|J_0|(1+\beta)$, so if β is large enough the first term will always be more important than the second and instability must occur.

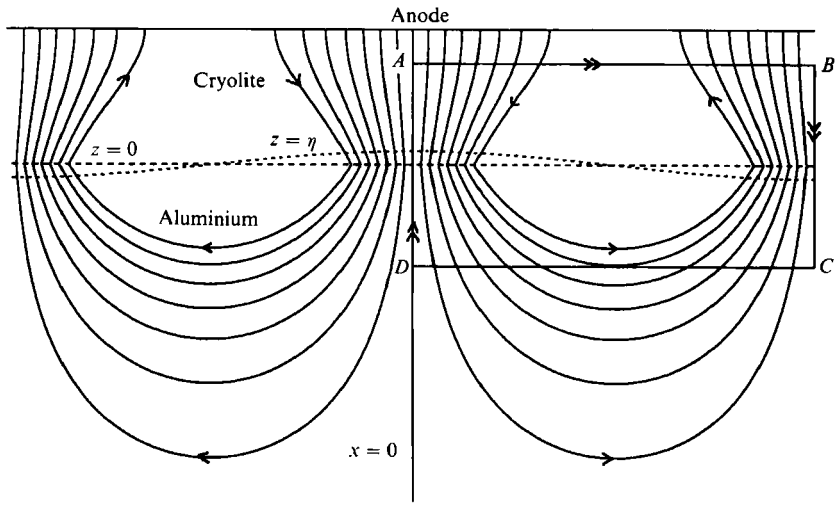

FIGURE 3. Fieldlines of the perturbed current flow $\boldsymbol{j}$.

To summarize, the electrical conductivity ratios are crucial in driving the instability. The mechanism relies on the fact that $\boldsymbol{j}$ is almost vertical in the cryolite, but has an important horizontal component in the aluminium. Once again the role of the far-field gradients is highlighted.

To conclude this section we note two other general characteristics of the instability which have a simple physical interpretation. First, instabilities occur at longer wavelengths, mainly because the stabilizing effects of surface tension and gravity are then weaker. The electromagnetic forces on the other hand either remain constant, or become stronger as the wavelength increases (see (4.12)). Secondly, increasing the depth of the aluminium pool is always stabilizing. The unstable wavelengths are typically much longer than H so the associated fluid motion always penetrates the entire pool depth. Thus, the deeper the pool, the greater the energy required to establish a wave.

7. Conclusions

We have modelled an aluminium reduction cell by uniform horizontal plane conducting layers of finite depth and infinite horizontal extent. In the undisturbed state the electric current is uniform and the magnetic field a linear function of position, and mechanical dissipation in the flow has been modelled by a linear frictional term. The propagation of plane waves across the layer is described by an anisotropic dispersion relation. Gravity, surface tension and friction are stabilizing, while the Kelvin–Helmholtz mechanism is always destabilizing. Electromagnetic effects may also be destabilizing at wavelengths of order 1 m or more, depending on the magnetic field gradients due to remote conductors. The most important destabilizing term arises from vertical gradients of the horizontal field components (or horizontal gradients of the vertical field).

The main limitations of this analysis are the uniform-current assumption, and infinite horizontal extent of the layer. In practice the horizontal current may change sign across the cell, but since the most important magnetic instability depends purely on the vertical current component J_z (which is approximately constant), this limitation may not be so serious. Although the dispersion relation is homogeneous,

the linearly varying magnetic field imposes a linear variation on the wave-induced flow (paper I). lateral boundaries (cell walls) must therefore have an important influence on stability, and this effect needs further study.

Appendix. Derivation of boundary conditions

We denote the current potential in layer i by Φ_i (note that layer 3 is the carbon anode and layer 4 the carbon cathode at the base of the aluminium pool):

$$\Phi_1 = J_0 z + J_H x + \phi_1 \quad \Phi_2 = J_0 z + (\sigma_2/\sigma_1) J_H x + \phi_2,$$
$$\Phi_3 = J_0 z + (\sigma_c/\sigma_1) J_H x + \phi_3, \quad \Phi_4 = J_0 z + (\sigma_c/\sigma_1) J_H x + \phi_4,$$

where σ_c is the electrical conductivity of carbon, and the ϕ_i are the perturbation current potentials. At each interface the normal current and tangential electric field must be continuous – i.e.

$$\nabla\Phi\cdot\hat{\boldsymbol{n}}, \quad \sigma^{-1}\nabla\Phi\times\hat{\boldsymbol{n}}, \tag{A 1a, b}$$

must be continuous across each interface.

A. 1. *Cryolite/anode interface*

Applying (A 1b),

$$\frac{1}{\sigma_c}\left(J_0\hat{\boldsymbol{z}} + \frac{\sigma_c}{\sigma_1} J_H \hat{\boldsymbol{x}} + \nabla\phi_3\right)\times\hat{\boldsymbol{n}} = \frac{1}{\sigma_2}\left(J_0\hat{\boldsymbol{z}} + \frac{\sigma_2}{\sigma_1} J_H \hat{\boldsymbol{x}} + \nabla\phi_2\right)\times\hat{\boldsymbol{n}}.$$

This simplifies to

$$\nabla\phi_2\times\hat{\boldsymbol{z}} = (\sigma_2/\sigma_c)\,\nabla\phi_3\times\hat{\boldsymbol{z}}.$$

Since $\sigma_2/\sigma_c \ll 1$, we approximate $\nabla\phi_2\times\hat{\boldsymbol{z}} = 0$ at $z = h_2$ to give (3.2).

A. 2. *Aluminium/cathode interface*

Applying (A 1b) we find

$$\frac{1}{\sigma_1}(J_H\hat{\boldsymbol{x}} + \nabla\phi_1)\times\hat{\boldsymbol{z}} = \frac{1}{\sigma_c}\left(\frac{\sigma_c}{\sigma_1} J_H\hat{\boldsymbol{x}} + \nabla\phi_4\right)\times\hat{\boldsymbol{z}},$$

and since $\sigma_c/\sigma_1 \ll 1$ we approximate

$$(\nabla\phi_4)_{z=-h_2}\times\hat{\boldsymbol{z}} = 0. \tag{A 2}$$

The cathode may be imagined to extend to infinity, in which case $\nabla\phi_4 \to 0$ as $z\to-\infty$, or (as assumed by Pigny & Moreau 1991) the cathode may have a lower plane surface on which the normal derivative of ϕ_4 vanishes. Either condition together with (A 2) implied that $\phi_4 = 0$. Then (A 1a) gives $\partial\phi_1/\partial z = 0$ at $z = -h_1$, which yields (3.3).

A. 3. *Aluminium/cryolite interface*

The unit normal at this interface is $\hat{\boldsymbol{z}} - \nabla\eta$, so (A 1$a$) gives

$$(J_0\hat{\boldsymbol{z}} + J_H\hat{\boldsymbol{x}} + \nabla\phi_1)\cdot(\hat{\boldsymbol{z}} - \nabla\eta) = \left(J_0\hat{\boldsymbol{z}} + \frac{\sigma_2}{\sigma_1} J_H\hat{\boldsymbol{x}} + \nabla\phi_2\right)\cdot(\hat{\boldsymbol{z}} - \nabla\eta).$$

The leading order in η this gives

$$\frac{\partial\phi_1}{\partial z} = \frac{\partial\phi_2}{\partial z} + J_H\frac{\partial\eta}{\partial x}\left(1 - \frac{\sigma_2}{\sigma_1}\right),$$

and using the approximation $\sigma_2/\sigma_1 \ll 1$ leads to (3.4).

Also at this interface (A 1*b*) gives

$$\frac{1}{\sigma_1}(J_0\hat{z}+J_H\hat{x}+\nabla\phi_1)\times(\hat{z}-\nabla\eta)=\frac{1}{\sigma_2}\left(J_0\hat{z}+\frac{\sigma_2}{\sigma_1}J_H\hat{x}+\nabla\phi_2\right)\times(\hat{z}-\nabla\eta).$$

To leading order in η:

$$\nabla(\phi_2+J_0\eta)\times\hat{z}=\frac{\sigma_2}{\sigma_1}\nabla(\phi_1+J_0\eta)\times\hat{z},$$

and again using the approximation $\sigma_2/\sigma_1 \ll 1$ leads to (3.5).

REFERENCES

Fraser, K. J., Billinghurst, D., Chen, K. L. & Keniry, J. T. 1989 Some applications of mathematical modelling of electric current distributions in Hall–Héroult cells. *Light Metals*, pp. 219–226.

Lympany, S. D., Evans, J. W. & Moreau, R. 1983 Magnetohydrodynamic effects in aluminium reduction cells. In *Proc. IUTAM Symp. on Metallurgical Applications of Magnetohydrodynamics, Cambridge, 1982*, pp. 15–23. London: The Metals Society.

Moreau, R. J. & Ziegler, D. 1986 Stability of aluminium cells: a new approach. *Light Metals*, pp. 359–364.

Murty, G. S. 1961 Instability of a conducting fluid slab carrying uniform current in the presence of a homogeneous magnetic field. *Ark. Fys.* **19**, 495.

Pigny, S. & Moreau, R. 1991 Stability of fluid interfaces carrying an electric current in the presence of a magnetic field. *Euro. J. Mech.* B (to appear).

Potočnik, V. 1989 Modelling of metal-bath interface waves in Hall–Héroult cells using ester/phoenics. *Light Metals*, pp. 227–235.

Sneyd, A. D. 1985 Stability of fluid layers carrying a normal electric current. *J. Fluid Mech.* **156**, 223–236 (referred to herein as paper I).

Urata, N. 1985 Magnetics and metal pad instability. *Light Metals*, pp. 581–589.